CHAPTER 5 The mean meridional circulation

5.1 The observed meridional transports of energy and moisture

As discussed in Chapter 3, moist static energy conservation is expressed by

$$\frac{Dh}{Dt} = g\frac{\partial}{\partial p}(R + F_h) \tag{5.1}$$

where

$$h \equiv c_p T + \phi + Lq \tag{5.2}$$

is the moist static energy. Using the methods discussed in Chapter 2, we can derive

$$\frac{1}{a\cos\varphi}\frac{\partial}{\partial\varphi}\int_0^{p_S}\left\{\overline{[v][h]}\cos\varphi + [\overline{v^* h^*}]\cos\varphi\right\}\frac{dp}{g} = [\overline{F_h} + \overline{R}]_S - [\overline{R_T}]\,. \tag{5.3}$$

Here the square brackets denote zonal means, R_T is the net radiation at the top of the atmosphere, and a time average has been used to eliminate the tendency term. Eq. (5.3) expresses the requirement of total energy balance for a "ring" of air along a latitude circle. By further integration of (5.3) with respect to latitude, we can obtain the meridional energy transport by the atmosphere, with dimensions of energy per unit time, much as we worked out the meridional energy transport by the atmosphere and ocean combined in Chapter 1, based on the net top-of-the-atmosphere radiation. Observations of this atmospheric total meridional energy transport are discussed below.

We can derive a corresponding equation for the "precipitable water," or vertically averaged water vapor amount, using essentially the same procedure again. The result is

$$\frac{1}{a\cos\varphi}\frac{\partial}{\partial\varphi}\int_0^{p_S}\left\{\overline{[v][q_v]}\cos\varphi + [\overline{v^* q_v^*}]\cos\varphi\right\}\frac{dp}{g} = \overline{[F_{q_v}]_S} - \int_0^{p_S}[\overline{C}]\frac{dp}{g}\ , \tag{5.4}$$

and the corresponding result for liquid water is

$$\frac{1}{a\cos\varphi}\frac{\partial}{\partial\varphi}\int_0^{p_S}\left\{\overline{[v][l]}\cos\varphi+[\overline{v^*l^*}]\cos\varphi\right\}\frac{dp}{g}=\overline{[F_l]_S}+\int_0^{p_S}[\overline{C}]\frac{dp}{g}-[\bar{P}]\quad,\qquad(5.5)$$

where

$$P\equiv r_S\qquad(5.6)$$

is the precipitation rate at the surface. For most purposes, (5.5) can be approximated by

$$[\bar{P}]=\int_0^{p_S}[\bar{C}]\frac{dp}{g},\qquad(5.7)$$

which simply says that the surface precipitation rate is equal to the vertically integrated condensation rate. Adding (5.4) and (5.5), we find that

$$\frac{1}{a\cos\varphi}\frac{\partial}{\partial\varphi}\int_0^{p_S}\left\{\overline{[v][q_v+l]}\cos\varphi+[\overline{v^*(q_v^*+l^*)}]\cos\varphi\right\}\frac{dp}{g}=\overline{[F_{q_v+l}]_S}-[\bar{P}]\quad,\qquad(5.8)$$

and for most purposes this can be approximated by

$$\frac{1}{a\cos\varphi}\frac{\partial}{\partial\varphi}\int_0^{p_S}\left\{\overline{[v][q_v]}\cos\varphi+[\overline{v^*q_v^*}]\cos\varphi\right\}\frac{dp}{g}=\overline{[F_{q_v}]_S}-\overline{[P]}\quad.\qquad(5.9)$$

Note that the meridional transport of total water has been approximated by the meridional transport of vapor.

The globally averaged evaporation and precipitation rates, which must balance in a time average, are not accurately known, but are roughly 3 kg m^{-2} day^{-1}. It follows that an average water molecule thus spends a "residence time" of about 8 days in the atmosphere between its introduction by surface evaporation, and its removal by precipitation. This means that if we average the vertically integrated moisture budget of the atmosphere over a time interval at least several times longer than 8 days, e.g. over one month or more, the local time rate of change term of (5.4) becomes negligible, and we obtain a balance between evaporation, precipitation, and the lateral flux of moisture into or out of the region. Strictly speaking, (5.4) applies to the time rate of change of the vertical integral of the *total* atmospheric moisture, including atmospheric liquid and ice, but recall that liquid and ice make only a tiny contribution to the total moisture content of the atmosphere. According to (5.9), when precipitation exceeds evaporation, moisture must be laterally "imported" by the atmosphere. When evaporation exceeds precipitation, the opposite occurs. The observed meridional transport of moisture is discussed below. For obvious reasons, it is convenient to discuss energy and moisture together.

Recall that the dry static energy satisfies $s = h - Lq$. Then (5.3) and (5.4) can be combined, with the use of (5.7), to derive a corresponding equation for the dry static energy:

$$\frac{1}{a\cos\varphi}\frac{\partial}{\partial\varphi}\int_0^{p_S}\left\{\overline{[v][s]}\cos\varphi + [\overline{v^* s^*}]\cos\varphi\right\}\frac{dp}{g} = [\overline{F_s} + \bar{R}]_S - [\overline{R_T}] + L[\bar{P}]\,. \qquad (5.10)$$

We now present some observations of the energy transports of the atmosphere and ocean as reported by Trenberth and Caron (2001) and Masuda (1988). Fig. 5.1 shows the

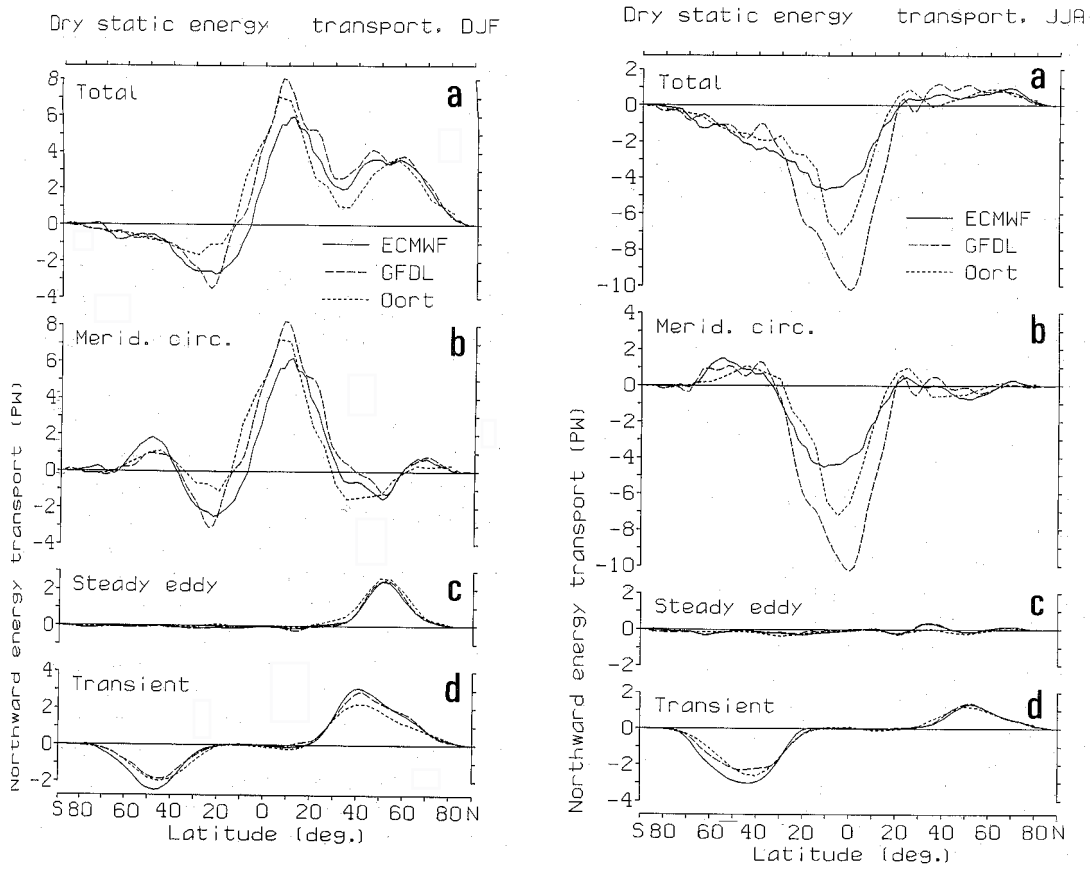

Figure 5.1: **a) Northward transport of dry static energy during DJF (December - January - February) in units of PW. (a) Total transport; (b) transport by the mean meridional circulation; (c) transport by stationary eddies; (d) transport by transient eddies. For all panels, the solid lines show the results obtained from ECMWF data, the dashed lines from GFDL data, and the dotted lines from Oort's (1983) statistics. Figure from Masuda (1988). b) Northward transport of dry static energy during JJA (June - July - August). From Masuda (1988).**

zonally integrated poleward transport of dry static energy for December, January, and February (DJF) and June, July, and August (JJA). The dry static energy transport can be

computed from the expression $(2\pi a\cos\varphi)\int_0^{p_S}\{[v][s]+[v^*s^*]\}\frac{dp}{g}$; compare with (5.10). The dimensions of the dry static energy transport are energy per unit time. The total dry static energy transport can be broken down into components associated with the mean meridional circulation (hereafter MMC), the stationary eddies, and the transient eddies.[1] The MMC dominates in the tropics. It gives weak equatorward fluxes in mid-latitudes of the winter hemispheres, due to the Ferrell Cells. The stationary eddies are significant in the Northern Hemisphere midlatitudes, particularly in winter, but not in the tropics or the Southern Hemisphere midlatitudes. The transient eddies are important in the middle latitudes of both hemispheres. In the Northern Hemisphere, they are noticeably more vigorous in DJF than in JJA, but there is relatively little seasonal change in the Southern Hemisphere.

Fig. 5.2 shows the corresponding results for "latent energy transport;" this quantity is

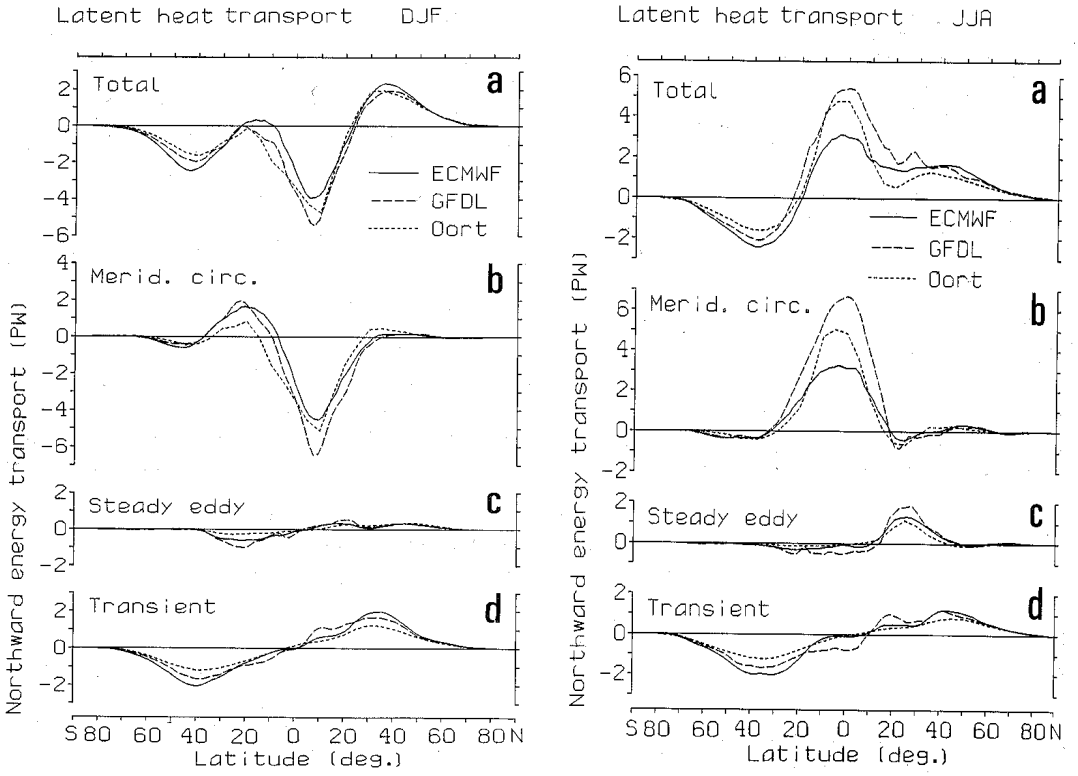

Figure 5.2: a) Northward transport of latent energy during DJF (December-January-February). b) Northward transport of latent energy during JJA (June-July-August). From Masuda (1988).

closely related to the zonally averaged difference between precipitation and evaporation, as shown by (5.9). Again the mean meridional circulation dominates in the tropics. Note also that in the tropics the latent energy transport is away from the poles, as discussed earlier.

[1] Masuda refers to the stationary eddies as "steady eddies." As Dave Barry would say, "Steady Eddie and the Transients" would be a great name for a band.

Stationary eddy contributions are noticeable in the tropics, due to monsoon circulations there, but are not so important in middle latitudes. Keep in mind here that in the middle latitudes, particularly in winter, the lower temperatures imply that the atmosphere contains little water vapor, so that there cannot be much latent energy transport.

The sum of the dry static energy transport and the latent energy transport gives the moist static energy transport, which is, practically speaking, nearly the same as the total energy transport. The moist static energy transport is shown in Fig. 5.3, for each of the four seasons. These curves are relatively simple, and shaped roughly like $\sin(2\varphi)$. The northward

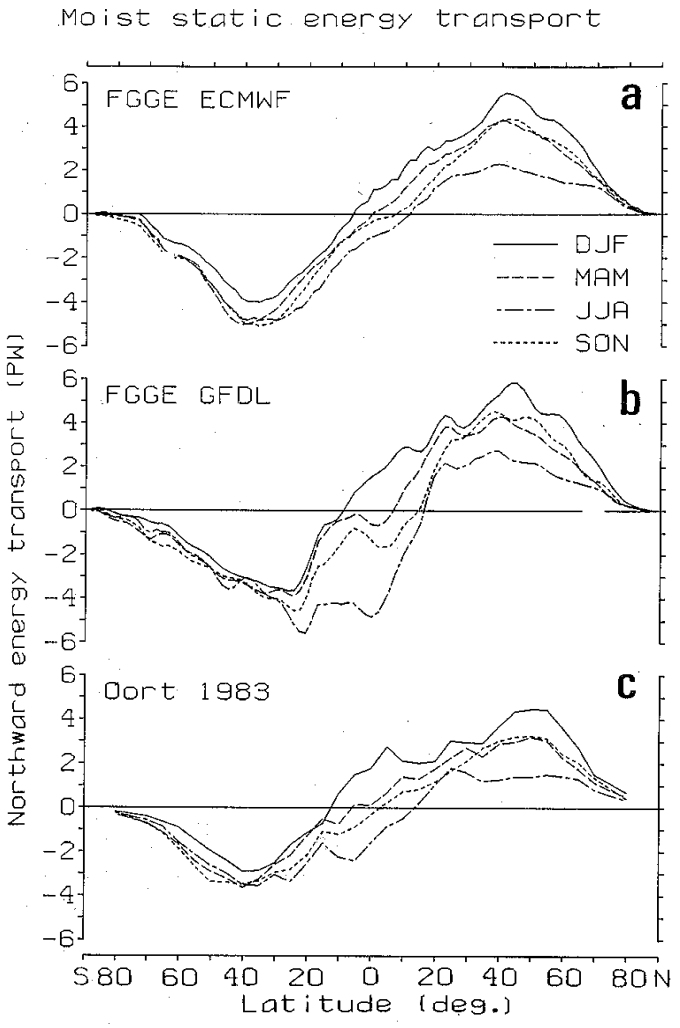

Figure 5.3: **Northward transport of moist static energy during the four seasons from the analyses of (a) ECMWF, (b) GFDL and (c) Oort (1983). The solid lines are for DJF, dashed lines for MAM, dash-dotted lines for JJA, and dotted lines for SON seasons. From Masuda (1988).**

flux of h increases northward from about 40°S to 40°N, implying that the atmosphere receives a net input of energy at its upper and/or lower boundaries, through this range of latitudes. The poleward transport shows a noticeable seasonal cycle in the Northern Hemisphere, with the strongest transport in DJF, but the Southern Hemisphere transport shows relatively little

seasonal change. Fig. 5.3 shows results from three different analyses, and there are significant differences among them. This illustrates that the observations are subject to serious uncertainties.

Fig. 5.4 shows the *annual mean* moist static energy transport, this time from six different analyses. The disagreements among the analyses suggest that the peak values in middle latitudes are uncertain by at least 25%. This is a very troubling discrepancy for such an important quantity as the annually averaged total energy transport by the atmosphere. Of course, the disagreements among the various analyses cannot necessarily be interpreted directly as uncertainties, because the different methods and/or data used may a priori be of different degrees of merit.

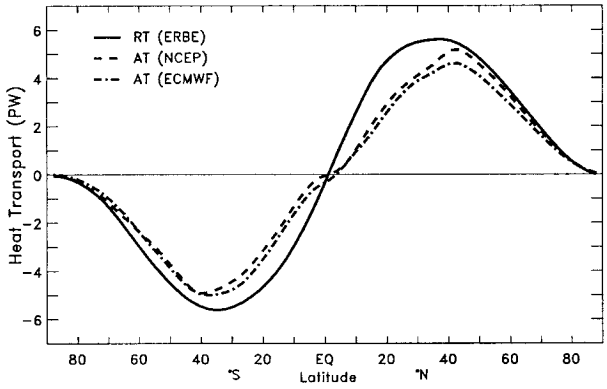

Figure 5.4: **The required annual - mean total heat transport from the TOA radiation (RT) is given along with the estimates of the total atmospheric transport (AT) from NCEP and ECMWF reanalyses. From Trenberth and Caron (2001).**

Fig. 5.5 breaks the annual mean moist static energy transport down into contributions by the MMC, the stationary eddies, and the transient eddies. Viewed in this annual mean sense, the MMC appears to play a small role, because its contributions in different seasons cancel, while the transient eddies and to a lesser extent the stationary eddies contribute consistently throughout the year, and so dominate the annual mean moist static energy transport. As the previous figures make clear, this picture is misleading. In reality, the MMC plays a very strong role in the total energy transport in the individual seasons.

We have already shown, in Chapter 1, the annual mean northward energy transport by the ocean and atmosphere combined; this quantity was first diagnosed by Vonder Haar and Oort (1973). The curve of the annually averaged total energy transport has a pleasingly simple shape. The maximum absolute values in middle latitudes of both hemispheres are on the order of 6 PW. This total energy transport by the climate system can be inferred directly from satellite measurements of the Earth's radiation budget, and so is known with relatively good accuracy now.

By subtracting the annually averaged atmospheric energy transport from the annually averaged total (atmosphere plus ocean) energy transport, it is possible to infer the annually averaged energy transport by the oceans, as a residual. This also was done by Vonder Haar and Oort (1973). The ocean energy transport is very difficult to determine directly from measurements of the ocean's temperature and currents, because of the lack of suitable data. In other words, we lack the data to work out the energy transport by the oceans using

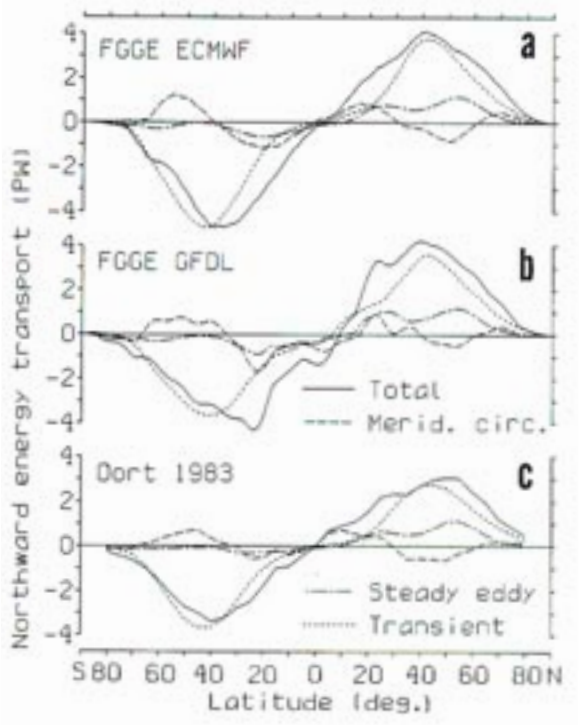

Figure 5.5: **Decomposition of the annual mean northward moist static energy transport (solid lines) derived from (a) ECMWF, (b) GFDL and (c) Oort's data into the contributions of the mean meridional circulation (dashed lines), stationary eddies (dash-dotted lines) and transient eddies (dotted lines). From Masuda (1988).**

methods analogous to those used to obtain the energy transport by the atmosphere.

Some results for the poleward transport of energy by the oceans are shown in Fig. 5.6. These curves were obtained by the "residual" method described above. One direct, "hydrographic" estimate (due to Bennett, 1978) is also shown in the figure, however. The peak ocean energy transports are on the order of 30 to 40% of the total transport by the atmosphere and ocean combined; in other words, the oceans appear to make a very significant contribution to the total poleward energy transport by the climate system. Fig. 5.7 summarizes the contributions of the ocean and atmosphere to the poleward energy transport.

5.2 A simple theory of the Hadley circulation

We now discuss a theory of an idealized mean meridional circulation, *without eddies*. Much of the discussion is based on the work of Held and Hou (1980), as summarized by Lindzen (1990). For this purpose, we temporarily adopt a simplified set of equations to describe the mean meridional circulation, as follows:

$$\nabla \bullet \mathbf{V} = 0, \tag{5.11}$$

$$\nabla \bullet (\mathbf{V}u) - \left(f + \frac{u \tan\varphi}{a}\right) v = \frac{\partial}{\partial z}\left(\nu \frac{\partial u}{\partial z}\right), \tag{5.12}$$

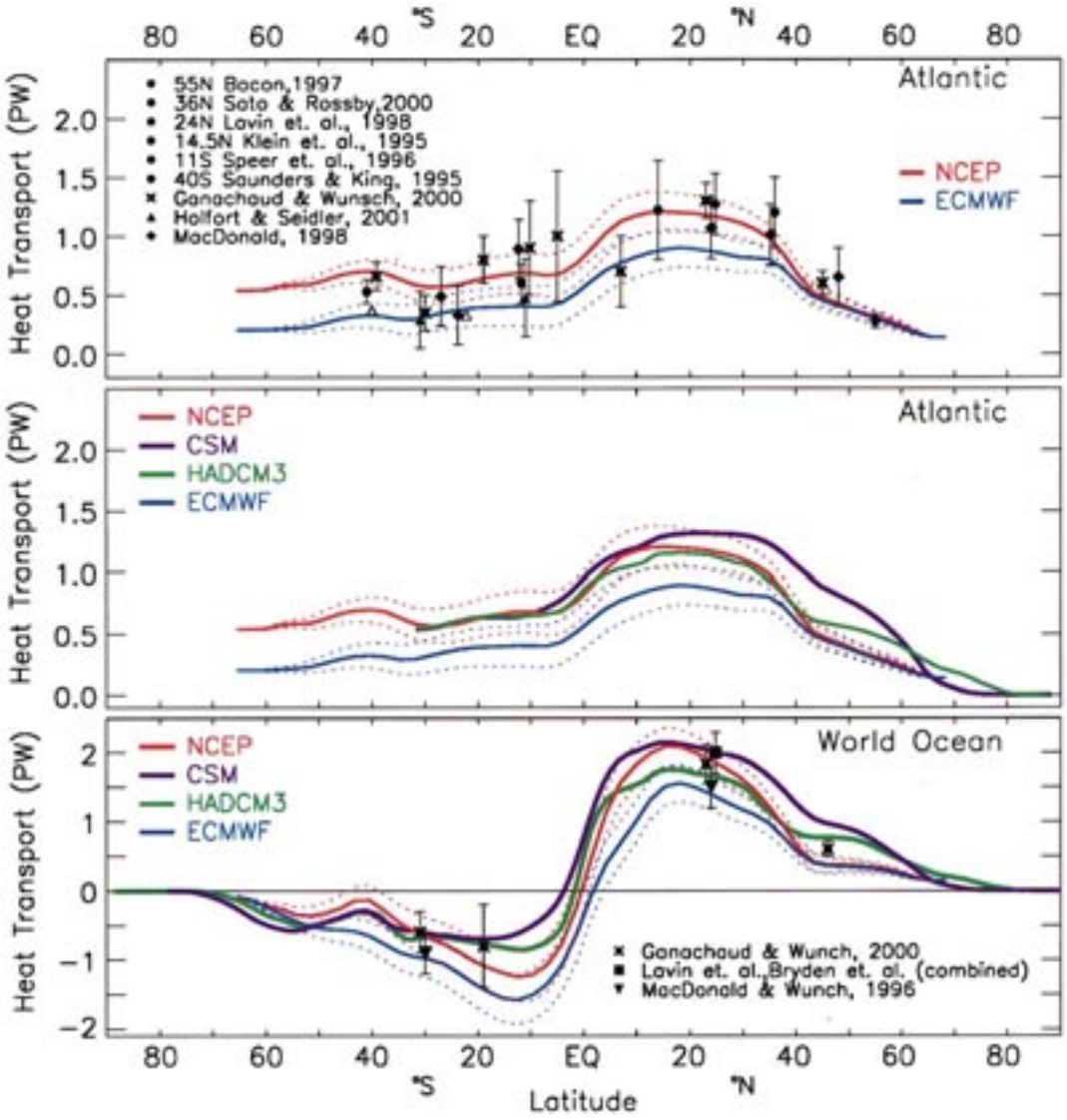

Figure 5.6: **The northward ocean heat transports from the NCEP-derived and ECMWF-derived products are compared (top) for the Atlantic Ocean with direct ocean estimates from sections, as identified in the key. The dashed curves show estimates of the uncertainty for the derived transports. Where given in the original source, error bars are also plotted and the symbol is solid. Slight offsets in latitude are introduced where overlap would otherwise occur. Several sections are not exactly along a latitude circle, notably those for Bacon (1997) at 55^{o}N and the Saunders and King (1995) section along 45^{o}S (South America to 10^{o}E) to 35^{o}S (Africa), plotted at 40^{o}S. (middle) Comparison of the derived results with transports from the simulations with a coupled ocean-atmosphere model called HADCM3 and another model called CSM for the Atlantic. (bottom) Results for the global ocean along with those from Macdonald and Wunsch (1996) at 24^{o}N and 30^{o}S, and at 24^{o}N the combined Lavin et al. (1998) and Bryden et al. (1991) and for Ganachaud and Wunsch (2000). From Trenberth and Caron (2001).**

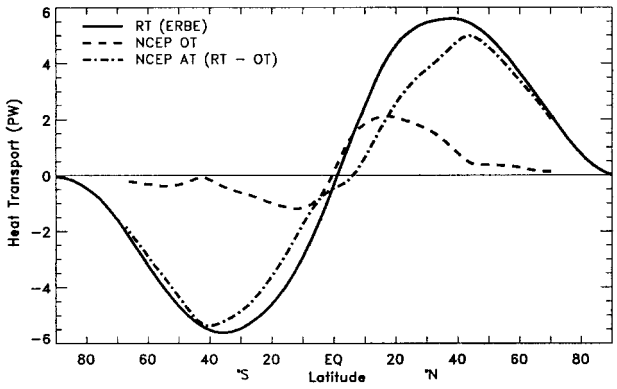

Figure 5.7: **The required total heat transport from the TOA radiation (RT) is compared with the derived estimate of the adjusted ocean heat transport (OT, dashed) and implied atmospheric transport (AT) from NCEP reanalyses. From Trenberth and Caron (2001).**

$$\nabla\bullet(\mathbf{V}v) + \left(f + \frac{u\tan\varphi}{a}\right)u = -\frac{1}{a}\frac{\partial\phi}{\partial\varphi} + \frac{\partial}{\partial z}\left(\nu\frac{\partial v}{\partial z}\right), \tag{5.13}$$

$$\nabla\bullet(\mathbf{V}\theta) = \frac{\partial}{\partial z}\left(\nu\frac{\partial\theta}{\partial z}\right) - \frac{(\theta - \theta_E)}{\tau}, \tag{5.14}$$

$$\frac{\partial\phi}{\partial z} = g\frac{\theta}{\theta_0}. \tag{5.15}$$

Here $\mathbf{V} = (v, \omega)$ is a two-dimensional vector in the latitude-height plane, $\phi = p/\rho_0$, and θ_0 and ρ_0 are constant "reference" values of the potential temperature and density, respectively. These equations are idealized, and require some explanation:

- We have assumed a steady state.
- We have assumed that there are no longitudinal variations whatsoever. One effect of this assumption is to eliminate the pressure gradient term of the equation of zonal motion.
- We are using the Bousinesq approximation for simplicity, so that the continuity equation reduces to non-divergence of the velocity field, and the hydrostatic equation reduces to the form given by (5.15).
- We have assumed that "friction" is due to downgradient mixing, with a non-negative and spatially constant mixing coefficient ν.

- We have assumed that there is a vertical mixing of potential temperature, with the same mixing coefficient as for momentum.
- We have assumed that the heating can be represented by "relaxation," with constant (positive) time scale τ, to an "equilibrium" potential temperature, θ_E, which can be thought of as the distribution of θ that would occur in radiative-convective equilibrium. Note that the symbol θ_E does *not* denote the equivalent potential temperature.

We simply specify θ_E, as follows:

$$\theta_E(\varphi, z) = \theta_0\left[1 - \Delta_H \sin^2\varphi + \Delta_V\left(\frac{z}{H} - \frac{1}{2}\right)\right]. \tag{5.16}$$

Here $\theta_0 \cong 400$ K is a reference potential temperature, $\Delta_H \cong 0.3$ is the fractional potential temperature drop (of the "radiative-convective equilibrium state") from the Equator to the pole, and $\Delta_V \cong 0.3$ is the potential temperature drop (again, of the "radiative-convective equilibrium state") from $z = H$ to the ground. We have to chose $\Delta_H \leq 1$ and $\Delta_V \leq 1$. For $\Delta_H > 0$, θ_E decreases towards the poles. For $\Delta_v > 0$, θ_E increases upward. A plot of θ_E is given in Fig. 5.8.

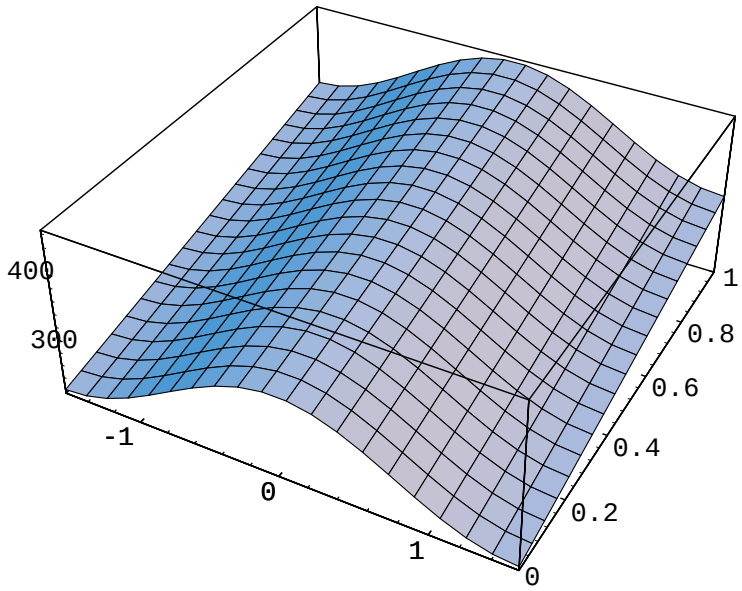

Figure 5.8: **A plot of θ_E (vertical axis) as a function of latitude in radians (front axis) and normalized height (right axis).**

As boundary conditions, we use

$$\frac{\partial u}{\partial z} = \frac{\partial v}{\partial z} = 0 \text{ at } z = H, \tag{5.17}$$

$$\frac{\partial \theta}{\partial z} = 0 \text{ at } z = H \text{ and } z = 0, \tag{5.18}$$

$$w = 0 \text{ at } z = H \text{ and } z = 0, \tag{5.19}$$

$$\nu \frac{\partial u}{\partial z} = Cu \text{ at } z = 0, \tag{5.20}$$

$$\nu \frac{\partial v}{\partial z} = Cv \text{ at } z = 0, \tag{5.21}$$

$$v = 0 \text{ at } \varphi = 0. \tag{5.22}$$

Here C is interpreted as a kind of "effective drag coefficient," which is actually the true drag coefficient times an average wind speed. Eqs. (5.20) and (5.21) thus represent linearizations of the bulk aerodynamic drag law discussed earlier; this is a simplifying assumption. Eq. (5.22) is a symmetry assumption, also made for simplicity, that allows us to restrict our analysis to a single hemisphere.

The model presented above allows a balanced, purely zonal flow if $\nu = 0$, i.e. if there is no friction. In this simple solution, $\theta = \theta_E$ everywhere, and the zonal wind is given by $u = u_E$, where, by definition, u_E satisfies

$$\frac{\partial}{\partial z}\left(f u_E + \frac{u_E^2 \tan\varphi}{a} \right) = -\frac{g}{a\theta_0}\frac{\partial \theta_E}{\partial \varphi}. \tag{5.23}$$

The boundary conditions (5.19) and (5.20) are not relevant in the absence of friction. If we use the lower boundary condition

$$u_E = 0 \text{ at } z = 0 \text{ for all } \varphi, \tag{5.24}$$

we find[2] that

$$\frac{u_E}{\Omega a} = \left[\left(1 + 2Ro_T \frac{z}{H} \right)^{1/2} - 1 \right] \cos\varphi, \tag{5.25}$$

where

[2] The use of (5.24) is somewhat awkward, because we have assumed no friction. Ordinarily we would attribute the weakness of the surface winds to the effects of surface drag.

$$Ro_T \equiv \frac{gH\Delta_H}{(\Omega a)^2} \tag{5.26}$$

is called the "thermal Rossby number." Eq. (5.25) describes a zonal velocity that becomes increasingly westerly with height at all latitudes, even over the Equator. A plot is given in Fig. 5.9.

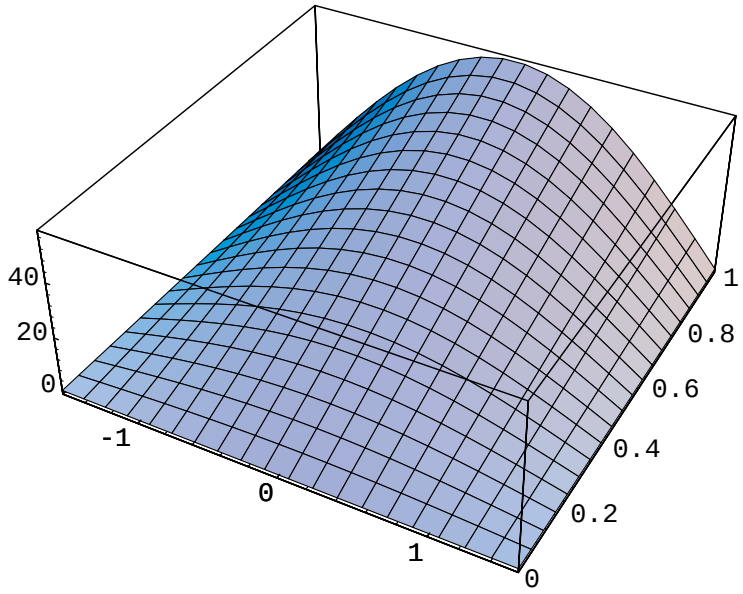

Figure 5.9: **A plot of u_E (vertical axis) as a function of latitude in radians (front axis) and normalized height (right axis).**

A physical interpretation of the thermal Rossby number is as follows. The thermal wind relation can be written as

$$\frac{\partial u}{\partial z} = -\frac{1}{f}\frac{g}{T}\frac{1}{a}\frac{\partial T}{\partial \varphi}, \tag{5.27}$$

which is analogous to

$$\frac{u_T}{H} \sim \frac{g}{\Omega}\frac{\Delta_H}{a}, \tag{5.28}$$

where u_T is the wind at the tropopause. A "Rossby number" can then be defined as

$$\frac{u_T}{\Omega a} = \frac{gH\Delta_H}{(\Omega a)^2}, \tag{5.29}$$

which agrees with (5.26). In short, the thermal Rossby number is a "regular" Rossby number (i.e. a wind scale divided by the product of the Coriolis parameter and the horizontal length scale), constructed using the wind at the tropopause (as the wind scale), divided by the product of the Earth's rotation rate (in the place of the Coriolis parameter) times the radius of the Earth (as the horizontal length scale). For the Earth's atmosphere,

$$Ro_T \cong 0.226 . \tag{5.30}$$

Let M_E be the angular momentum per unit mass associated with u_E:

$$M_E = a\cos\varphi(u_E + \Omega a\cos\varphi) . \tag{5.31}$$

From (5.25), we see that

$$\frac{M_E}{\Omega a^2} = \cos^2\varphi\left(1 + 2Ro_T\frac{z}{H}\right)^{1/2} . \tag{5.32}$$

Inspection of (5.32) shows that

$$\frac{M_E}{\Omega a^2} > 1 \text{ at the Equator.} \tag{5.33}$$

In fact, M_E has a maximum on the Equator, at $z = H$.

We now prove that with the "downgradient" momentum diffusion assumed here, a purely zonal circulation is impossible. This is called "Hide's theorem," after work by R. Hide. As a first step, we rewrite (5.12) as a conservation law for angular momentum, i.e.

$$\nabla\bullet(\mathbf{V}M) = \nabla\cdot(\nu\nabla M) , \tag{5.34}$$

where, as before, M is the angular momentum per unit mass. We have introduced two-dimensional eddy mixing for generality. Suppose that M has a maximum somewhere in the interior of the atmosphere. We can draw a contour of constant M around this maximum, in the (φ, z) plane. If we integrate over the region enclosed by this contour, the advection term on the left-hand side of (5.34) must integrate to zero, because of (5.11). The friction term on the right-hand side will represent a sink of M, however, because we have assumed that M is a maximum inside the contour. This means that (5.28) cannot be satisfied in this case, and we conclude that our assumption of a maximum of M inside the atmosphere is not tenable. For a similar reason, M cannot have a minimum inside the atmosphere.

Suppose now that M has a maximum at the Earth's surface. Again we can draw a contour of constant M around this maximum and close it off along the Earth's surface. As before, we can conclude, through the use of (5.11), that the advective term of (5.34) must vanish when integrated over the area enclosed by this contour. Friction with the air outside the

contour will still represent a sink of angular momentum, so the only chance for balance is if there is a *source* of angular momentum through drag with the Earth's surface. Such a source can only occur where the surface winds are easterly.

Similarly, using (5.17), we can show that M cannot have a maximum at $z = H$.

We thus conclude that, in the absence of eddies and with downgradient momentum transfer, *any maximum of M must occur at the Earth's surface in a region of easterlies*. This is observed, as can be seen in the plots of M presented in Chapter 2.

We have already worked out that in the absence of a mean meridional circulation, u will satisfy (5.25), which means that M will increase upward at all latitudes including the Equator. This violates our conclusion above that M can have a maximum only at the Earth's surface in a region of easterlies -- a conclusion that was reached based on the assumption of non-zero friction. We can conclude, therefore, that the solution given by (5.25) cannot apply if there is any friction in the system. In other words, *the existence of friction guarantees that there will be a mean meridional circulation*.

In particular there will have to be a Hadley circulation. When friction is present, the zonal wind given by $u = u_E$ is unrealistically strong, because the meridional rate of change of potential temperature given by $\theta = \theta_E$ is unrealistically rapid. A Hadley circulation makes the solution more realistic, because it transports heat poleward, thus reducing θ near the Equator, and increasing it at higher latitudes. The zonal wind decreases, accordingly.

Held and Hou further simplified their model in order to obtain approximate solutions analytically. Assuming conservation of angular momentum at the tropopause gives

$$u(\varphi, H) = \frac{\Omega a \sin^2\varphi}{\cos\varphi} . \tag{5.35}$$

Gradient balance tells us that

$$fu(H) + \frac{\tan\varphi}{a} u^2(H) = -\frac{1}{a}\frac{d}{d\varphi}\phi(H) . \tag{5.36}$$

The geopotential on the right-hand side of (5.36) can be evaluated by using the hydrostatic equation, giving

$$\frac{\phi(H)}{H} = g\frac{\hat{\theta}}{\theta_0} , \tag{5.37}$$

where the hat denotes a vertical mean. We can eliminate $u(H)$ in (5.36) by using (5.35), leading to

$$f\left(\frac{\Omega a \sin^2\varphi}{\cos\varphi}\right) + \frac{\tan\varphi}{a}\left(\frac{\Omega a \sin^2\varphi}{\cos\varphi}\right)^2 = -\frac{1}{a}\frac{d}{d\varphi}\left(gH\frac{\hat{\theta}}{\theta_0}\right). \tag{5.38}$$

This is a first-order ordinary differential equation for $\hat{\theta}$. It can be integrated to yield

$$\hat{\theta}(\varphi) = \hat{\theta}(0) - \frac{\theta_0}{2gH}\left(\frac{\Omega a \sin^2\varphi}{\cos\varphi}\right)^2. \tag{5.39}$$

Now suppose that beyond the poleward edge of the Hadley circulation, i.e. for latitudes $\varphi > \varphi^*$, the temperature is in radiative-convective equilibrium. We assume that the temperature is continuous at $\varphi = \varphi^*$. Then

$$\hat{\theta}(\varphi^*) = \hat{\theta}_E(\varphi^*). \tag{5.40}$$

Finally, we note that the Hadley circulation is an advective process, and so merely redistributes the potential temperature, without changing its average value, so that

$$\int_0^{\varphi^*} \hat{\theta}\cos\varphi d\varphi = \int_0^{\varphi^*} \hat{\theta}_E \cos\varphi d\varphi. \tag{5.41}$$

Substituting into (5.40) and (5.41) from (5.39) and (5.16), we get

$$\hat{\theta}(0) - \frac{\theta_0}{2gH}\left(\frac{\Omega a \sin^2\varphi^*}{\cos\varphi^*}\right)^2 = \theta_0(1 - \Delta_H \sin^2\varphi^*), \tag{5.42}$$

and

$$\begin{aligned}\int_0^{\varphi^*} \left[\hat{\theta}(0) - \frac{\theta_0}{2gH}\left(\frac{\Omega a \sin^2\varphi}{\cos\varphi}\right)^2\right]\cos\varphi d\varphi \\ = \int_0^{\varphi^*} \theta_0(1 - \Delta_H \sin^2\varphi)\cos\varphi d\varphi .\end{aligned} \tag{5.43}$$

Eqs. (5.42) and (5.43) can be solved as two equations for the two unknowns φ^* and $\hat{\theta}(0)$. For $\varphi^* \ll 1$, we find that

$$\varphi^* \cong \sqrt{\frac{5}{3}Ro_T}. \tag{5.44}$$

This gives $\varphi^* \cong 35°$, which is close to the right answer. Recall that Ro_T varies as the inverse square of the rotation rate. The theory predicts, therefore, that strongly rotating planets will have Hadley cells that are tightly confined near the Equator, while slowly rotating planets will have Hadley cells that extend out further towards the poles. This prediction is discussed further in the next section.

5.3 Extension to other planetary atmospheres

Williams (1988) explored the sensitivity of the general circulation to the planetary rotation rate, using a numerical model originally developed to simulate the general circulation of the Earth's atmosphere. The model is based on equations similar to those discussed in Chapters 2 and 3, with parameterizations of radiation, moist convection, and surface fluxes due to turbulence. Williams modified the model so that the lower boundary is a global ocean of zero heat capacity, and he ignored the possibility that the ocean could freeze. The insolation was prescribed to be the observed annual mean, and the distribution of cloudiness was prescribed to crudely mimic the observed cloudiness of the Earth. The model does not include a diurnal cycle, so that the sun is essentially a bright "torus" encircling the planet, rather than a point in the sky on the day-side of the planet; this idealization may be acceptable for sufficiently rapid rotation rates, but leads to obvious problems of interpretation for very slow rotation rates.

Williams performed a suite of extended numerical simulations in which the model adjusted to the rotation rate specified in each case. He measured the rotation rate in terms of

$$\Omega^* \equiv \frac{\Omega}{\Omega_E}, \tag{5.45}$$

where Ω is the rotation rate of the hypothetical planet being simulated, and Ω_E is the rotation rate of the Earth. A real planet that rotates much more slowly than Earth is Venus. A real planet that rotates more rapidly than Earth is Jupiter.

Fig. 5.10 shows the latitude-height distribution of the zonally averaged zonal wind, for values of Ω^* ranging from 0 to 8. Look first at the panel corresponding to $\Omega^* = 1$, i.e. Earth-like conditions. We see a westerly jet at a latitude of 30°, and with peak strength on the order of 50 m s^{-1}, which is comparable to what is observed on Earth. We also see easterlies in the tropics and at high latitudes. The solution is in fact reasonably Earth-like, even though the effects of mountains, etc., have been completely omitted from the model.

As Ω^* decreases towards zero, the jet moves poleward, ultimately disappearing in the limit of no rotation. As Ω^* increases to 8, the westerly jet moves in towards the Equator.

Fig. 5.11 shows the stream function of the mean meridional circulation, for various values of Ω^*. Not surprisingly, the case of $\Omega^* = 1$ produces an Earth-like Hadley circulation, consistent with the westerly jet noted above. As the rotation rate decreases, the Hadley cell broadens. In the limit of no rotation it extends all the way to the pole. As the rotation rate increases, the Hadley cell contracts towards the Equator, and additional cells appear in middle and higher latitudes. The dependence of the latitudinal extent of the Hadley cell on the rotation rate is broadly consistent with the theory of Held and Hou (1980), as discussed in the previous subsection. The additional cells that appear at higher rotation rates are reminiscent of the many zonal bands that appear in pictures of Jupiter.

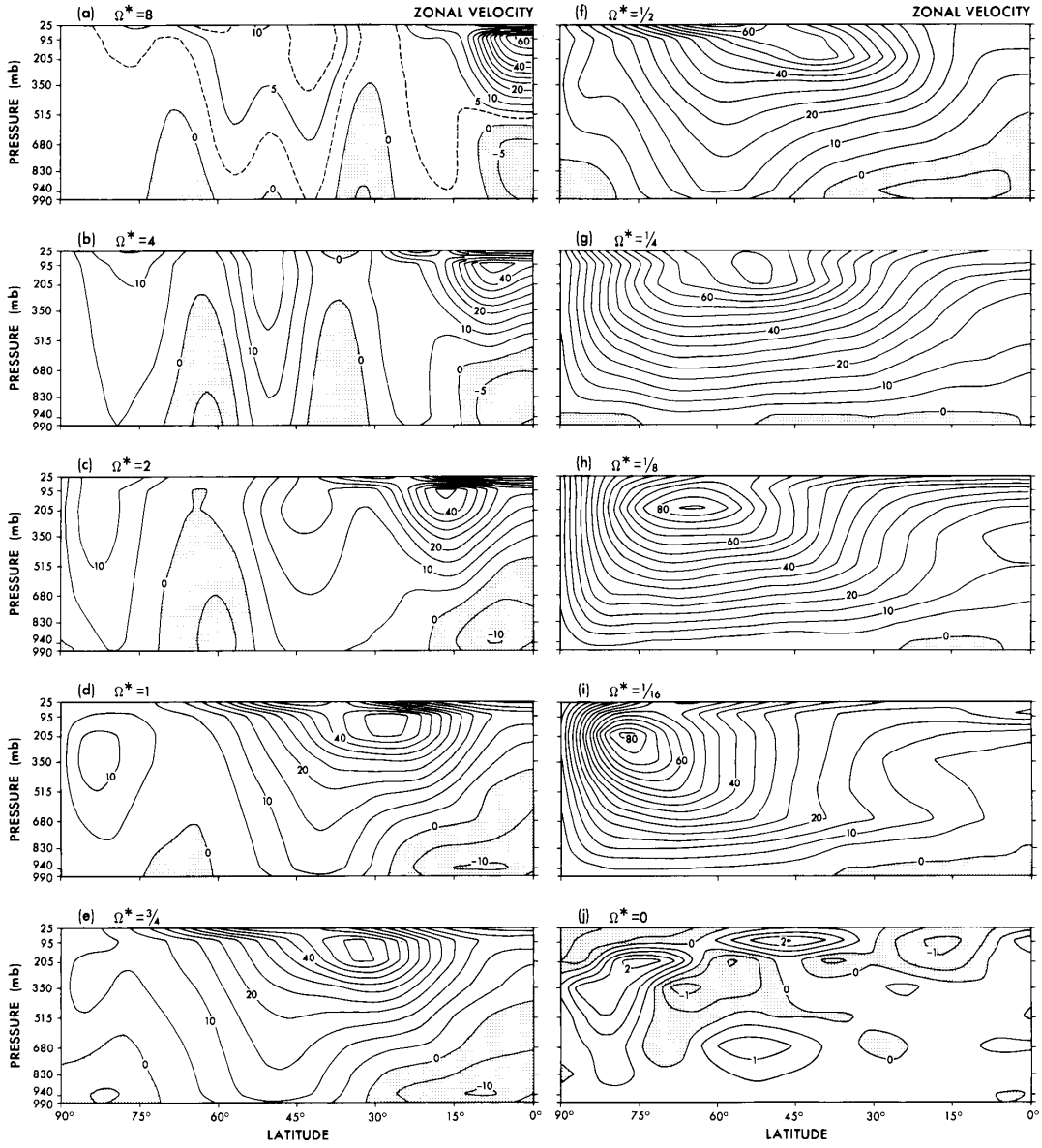

Figure 5.10: **The latitude-height distribution of the zonal mean zonal wind, in m s^{-1}, for various values of the rotation parameter. From Williams (1988).**

Fig. 5.12 shows the latitude-height cross section of the temperature, for various values of Ω^*. The meridional temperature gradient is strong on rapidly rotating planets, and weak on slowly rotating planets. Rotation evidently interferes with efficient poleward transport of energy. It does so by restricting the latitudinal excursions of particles, as discussed in Chapter 3.

Finally, Fig. 5.13 shows the latitude-height cross section of the eddy kinetic energy,

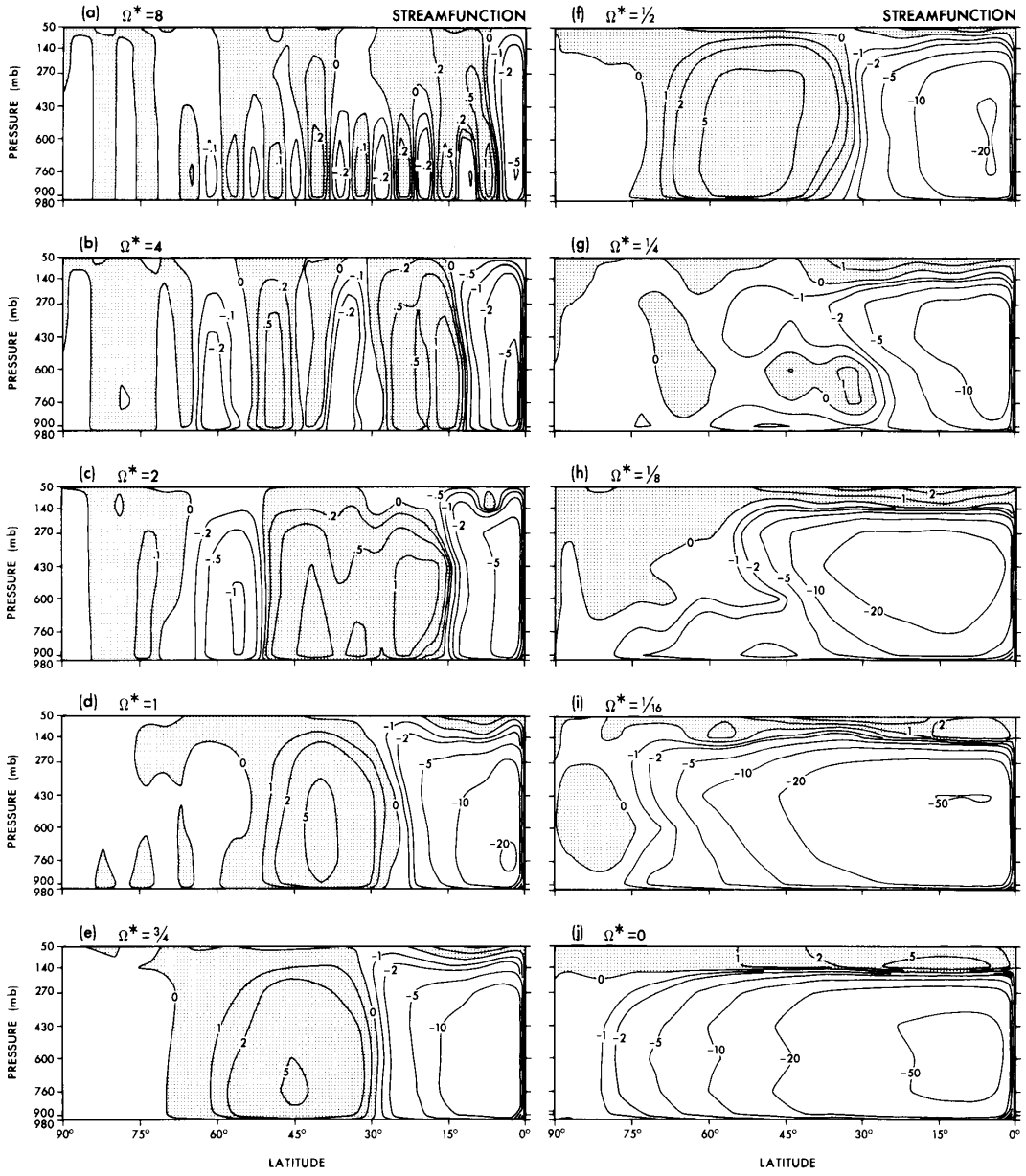

Figure 5.11: **The stream function of the mean meridional circulation, in 10^{10} kg s^{-1}, for various values of the rotation parameter. From Williams (1988).**

for various values of Ω^*. The exact definition of this quantity and the nature of its sources and sinks will be discussed in detail later; for now we simply note that it is a measure of the vigor of circulations that have longitudinal structures and arise, in these simulations, primarily from baroclinic instability. An interesting point is that the maximum eddy kinetic energy occurs for $\Omega^* = 1$; planets that rotate either more rapidly or less rapidly thank Earth have less vigorous eddies, by this measure. Apparently the Earth's rotation rate is just what is

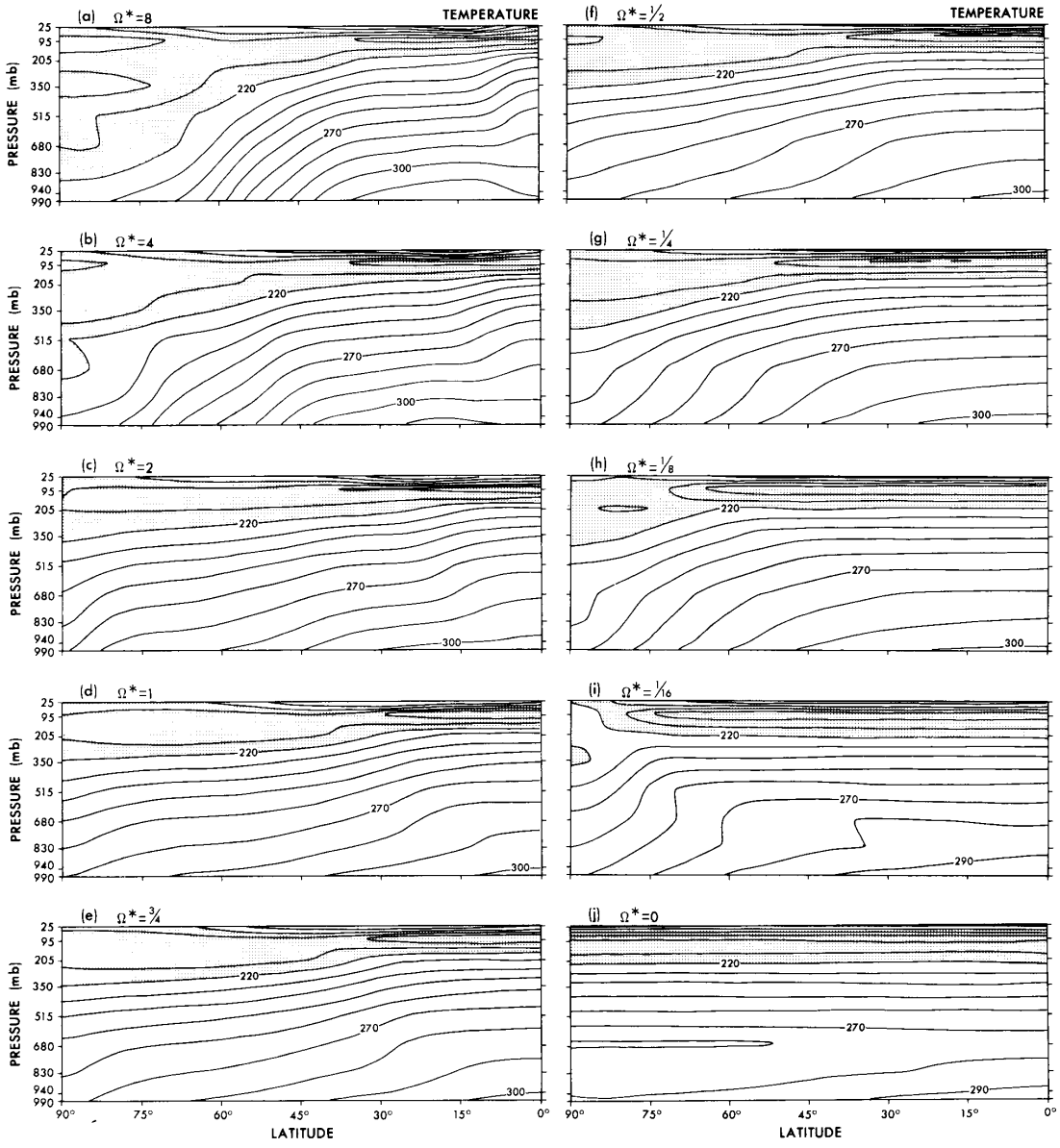

Figure 5.12: The latitude - height distribution of the temperature, in K, for various values of the rotation parameter. From Williams (1988).

needed to maximize the storminess of the middle latitudes! The Earth is the stormiest of all possible planets — a meteorologist's paradise.

5.4 Particle trajectories on the sphere: A partial explanation of "bandedness"

The bandedness of the circulation can be partially interpreted as a simple consequence of kinetic energy conservation in combination with angular momentum conservation. In

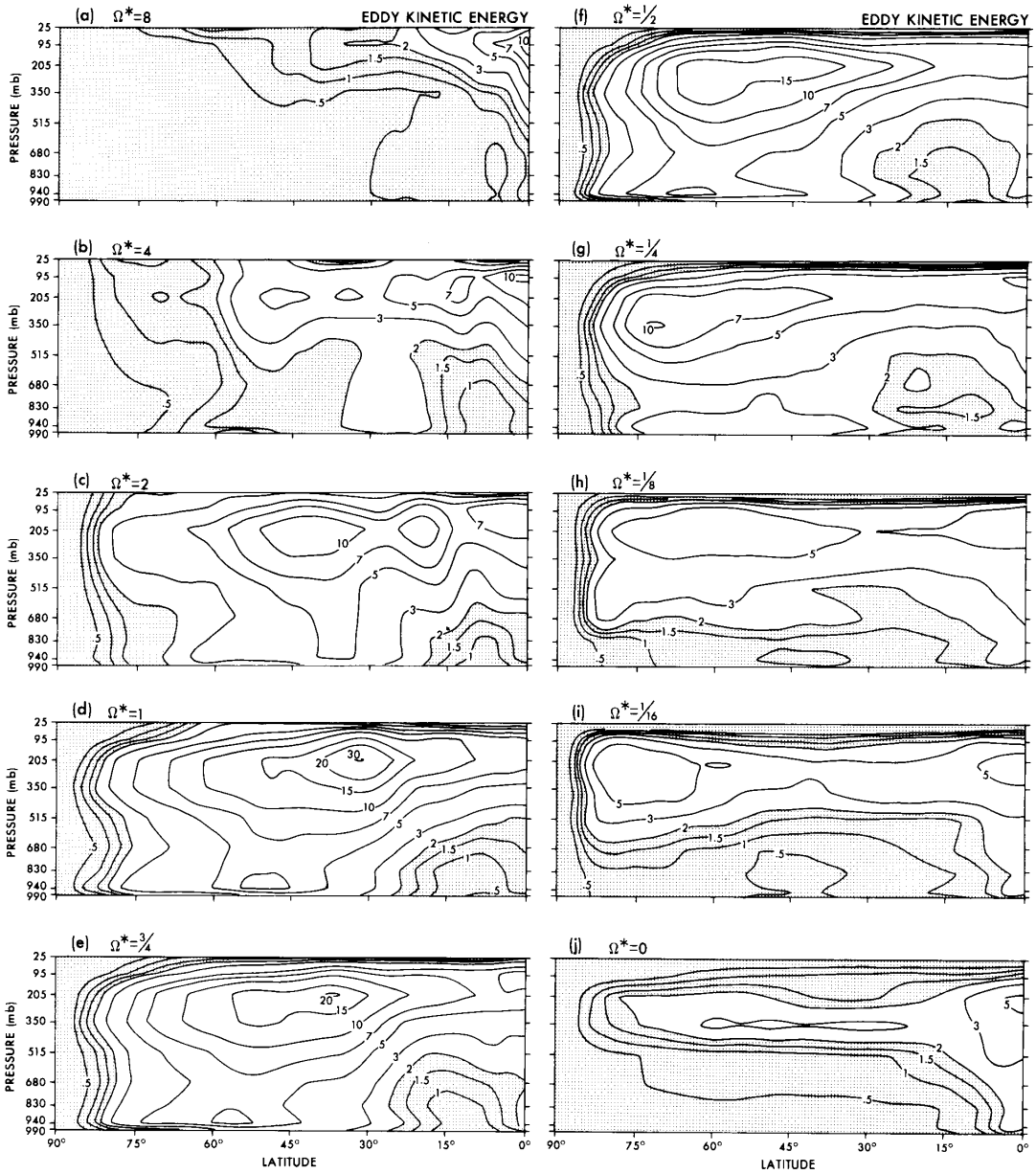

Figure 5.13: **The latitude - height distribution of the eddy kinetic energy, per unit mass, in m^2 s^{-2}, for various values of the rotation parameter. From Williams (1988).**

combination, angular momentum conservation and kinetic energy conservation imply some very strong constraints on the motion of particles on a spherical surface (Cushman-Roisin, 1982; Paldor and Killworth, 1988; Pennell and Seitter, 1990). To see this, consider the motion of a particle in the absence of pressure forces and friction. The equations of motion for the particle are simply:

$$\frac{Du}{Dt} = \left(f + \frac{u\tan\varphi}{a}\right)v,$$
$$\frac{Dv}{Dt} = -\left(f + \frac{u\tan\varphi}{a}\right)u \quad . \tag{5.46}$$

It follows from (5.46) that the kinetic energy K and the angular momentum M of the particle do not vary as it moves:

$$K = \frac{1}{2}(u^2 + v^2) = \frac{1}{2}s^2 = \text{constant} , \tag{5.47}$$

$$M = (\Omega a\cos\varphi + u)a\cos\varphi = \text{constant} . \tag{5.48}$$

In (5.47) s is the speed of the particle. Solving (5.48) for u, we find that

$$u = \frac{M - \Omega a^2\cos^2\varphi}{a\cos\varphi} . \tag{5.49}$$

You should be able to see from (5.46) that if a particle starts on the Equator with $v = 0$, it will remain on the Equator for all time, simply because $f + \frac{u\tan\varphi}{a} = 0$ there.

As a more interesting example, suppose that $u = 0$ at the Equator. Then (5.48) leads to

$$u = \Omega a\left(\frac{1 - \cos^2\varphi}{\cos\varphi}\right) \geq 0 . \tag{5.50}$$

From this result, it appears that $u \to \infty$ as $\varphi \to \frac{\pm\pi}{2}$. Recall, however, that K is also conserved. It follows that $|u| \leq s$. This implies that there is a maximum value of $|\varphi|$ beyond which the particle cannot go; the particle is confined within a ring centered on the Equator. At the north and south edges of the ring, $u = s$, $v = 0$, and $|\varphi| = \varphi_{max}$. See Fig. 5.14.

We now demonstrate that in general a particle's motion is confined within a range of latitudes. We allow an arbitrary choice of the initial latitude and velocity. Without loss of generality, assume that

$$\Omega > 0 . \tag{5.51}$$

Let

$$y \equiv \cos\varphi , \tag{5.52}$$

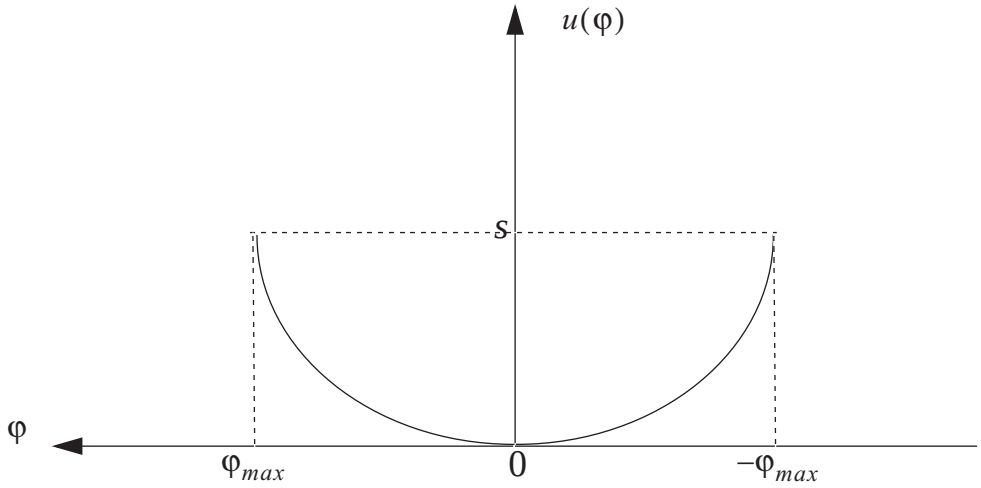

Figure 5.14: **Sketch illustrating the variation of the zonal wind with latitude under conservation of angular momentum, for the special case in which the zonal wind vanishes at the Equator.**

and note that

$$0 \le y \le 1 . \tag{5.53}$$

As the particle moves, its latitude changes so long as $v \neq 0$; its meridional motion is blocked where $v = 0$, i.e., it cannot cross a latitude where $v = 0$. In view of (5.47), at a latitude where $v = 0$ we have either $u = s$ or $u = -s$. Consider these two possibilities one at a time. In the first case, (5.48) reduces to

$$y_1^2 + xy_1 - \mu = 0 , \tag{5.54}$$

while in the second case we get

$$y_2^2 - xy_2 - \mu = 0 . \tag{5.55}$$

Here

$$x \equiv \frac{s}{\Omega a} > 0 \text{ and } \mu \equiv \frac{M}{\Omega a^2} . \tag{5.56}$$

Note that x and μ do not change as the particle moves around; they are "invariants of the motion." For the Earth's atmosphere, $\mu > 0$ in virtually every conceivable situation. In principle, however, it would be possible to have $\mu < 0$.

The solutions of (5.54) and (5.55) are

$$y_1 = -\frac{1}{2}x + \sqrt{\frac{1}{4}x^2 + \mu}\,, \tag{5.57}$$

and

$$y_2 = \frac{1}{2}x + \sqrt{\frac{1}{4}x^2 + \mu}\,, \tag{5.58}$$

respectively. In both cases, we have chosen the plus sign before the discriminant in order to satisfy $y > 0$. From (5.56) and (5.58) we see that

$$\frac{1}{4}x^2 + \mu = \frac{\frac{1}{4}v^2 + \left(\frac{1}{2}u + \Omega a\cos\varphi\right)^2}{(\Omega a)^2} \geq 0\,, \tag{5.59}$$

which implies that y_1 and y_2 are real numbers.

By subtracting (5.57) from (5.58), we obtain

$$y_2 - y_1 = x > 0\,. \tag{5.60}$$

This is a measure of the *width of the latitude band* within which the particle is confined. *Rotation inhibits latitudinal excursions larger than* $\cos^{-1}\left(\frac{s}{\Omega a}\right)$. As the rotation rate increases, $y_2 - y_1$, decreases. From (5.60) we see that y_2 is always greater than y_1. This means that y_2 corresponds to the latitude closer to the Equator (in either hemisphere), and y_1 corresponds to the latitude further from the Equator.

From (5.57) we can show that the condition for $y_1 = 0$ is simply $\mu = 0$, i.e. the particle has no angular momentum. A particle without angular momentum can reach the poles. A particle with $\mu \neq 0$ will never visit the poles.

From (5.58), we can show that $y_2 > 1$ is equivalent to

$$x + \mu > 1\,. \tag{5.61}$$

When $y_2 > 1$, i.e., when (5.61) is satisfied, a particle moving towards the Equator will not encounter a latitude where $v = 0$; it can therefore cross the Equator, and in fact it will keep moving until it reaches the latitude where $y = y_1$ in the opposite hemisphere. In such a case, the particle is confined in the vicinity of the Equator. We can say that the particle is "equatorially trapped."

When (5.61) is not satisfied, a particle moving toward the Equator will encounter a latitude $y = y_2$ where $v = 0$ before it gets to the Equator. The particle will, therefore, stop short of the Equator, i.e,. it will spend eternity in one hemisphere.

Since x decreases as the rotation rate increases, (5.60) suggests that rotation inhibits the latitudinal excursions of a particle undergoing inertial motion, i.e., rotation effectively confines the particle to a limited range of latitudes. To explore this further, consider first the case in which the particle's motion is confined to one hemisphere. In terms of meridional distance,

$$\begin{aligned} a(\varphi_1 - \varphi_2) &= a(\cos^{-1} y_1 - \cos^{-1} y_2) \\ &\cong \frac{a(y_1 - y_2)}{\sqrt{1 - \left(\frac{y_1 + y_2}{2}\right)^2}} \\ &= \frac{ax}{\sqrt{1 - \left(\frac{1}{4}x^2 + \mu\right)}} \quad . \end{aligned} \tag{5.62}$$

The approximation on the second line of (5.62) is valid when the band is sufficiently narrow. From (5.59), we can show that, for meteorologically relevant values of u and v,

$$\frac{1}{4}x^2 + \mu \cong \cos^2\varphi \, . \tag{5.63}$$

Substituting (5.63) into (5.62), we find that

$$a(\varphi_1 - \varphi_2) \cong \frac{ax}{\sin\varphi} = \frac{s}{\Omega \sin\varphi} = \frac{2s}{f} \, . \tag{5.64}$$

Here φ should be interpreted as a latitude in the middle of the particle's "band." We do not need to worry about division by zero in (5.64), because we are considering the case in which the particle's motion is confined to one hemisphere.

Now consider the case in which the particle is equatorially trapped. Then the width of the particle's band is given by

$$\begin{aligned} 2a\varphi_1 &= 2a\cos^{-1} y_1 \\ &= 2a\cos^{-1}\left(-\frac{1}{2}x + \sqrt{\frac{1}{4}x^2 + \mu}\right) . \end{aligned} \tag{5.65}$$

Using (5.63), this can be approximated as

$$2a\varphi_1 = 2a\cos^{-1}\left(-\frac{1}{2}x + \cos\varphi\right)$$
$$\cong 2a\cos^{-1}\left(1 - \frac{s}{2\Omega a}\right). \tag{5.66}$$

Here we have used (5.56) and the approximation $\cos\varphi \cong 1$, which is appropriate for equatorially trapped particles. Since $\cos x \cong 1 - \frac{x^2}{2}$, we can simplify (5.66) to

$$2a\varphi_1 \cong 2a\sqrt{\frac{s}{\Omega a}} = 2\sqrt{\frac{sa}{\Omega}}. \tag{5.67}$$

This is similar to the "Rhines length," $\sqrt{\frac{s}{\beta}}$, where $\beta \equiv \frac{1}{a}\frac{df}{d\varphi}$, which will be discussed in a later chapter.

It is clear from (5.64) and (5.67) that faster rotation confines the motion of a particle to a narrower latitudinal band. We can interpret this as a partial explanation for the results of Williams' numerical experiments, which show that more "bands" occur as the planetary rotation rate increases. When there are more bands, each band is narrower, and particles moving within a band are confined to a narrower range of latitudes.

The simple analysis given above is useful for interpretation of the observed mean meridional circulation. Nevertheless it is important to keep in mind that this analysis is highly idealized and has only limited relevance to the atmospheric circulation. A key simplifying assumption made above is that no pressure-gradient forces act on the moving particles. Notice that it would be possible for two of our inertially moving particles to collide. In the atmosphere, such collisions are prevented by the pressure-gradient force, which acts as a kind of "air-traffic control."

5.5 Summary

We discussed the energy balances of the atmosphere and ocean, which imply meridional transports of energy by the circulations of the atmosphere and ocean. The transports were dissected to show the contributions of the mean meridional circulation, the transient eddies, and the stationary eddies. We also separated out the transports of dry static energy and latent energy.

This was followed by a discussion of the theory of a zonally symmetric circulation, following Held and Hou (1980). Finally, we examined the numerical simulations of Williams (1988), which show how the mean meridional circulation varies as the planetary rotation rate is changed.

Problems

1. To estimate the width of the Hadley Cell, we used Eq. (5.40), which states that the temperature is continuous at the edge of the cell. Repeat the analysis, assuming

instead that the zonal wind is continuous. Compare the results obtained with these two assumptions.

2. Consider an air parcel at rest at the sea surface on the Equator. If the parcel rises from the surface to an altitude of 15 km, conserving its angular momentum, what is its zonal velocity? For purposes of this problem, define the axial component of the angular momentum by

$$M \equiv r\cos\varphi(\Omega r\cos\varphi + u)\,, \tag{5.68}$$

where r is the radial distance of the parcel from the center of the Earth.

3. Look up the information that you need to determine the thermal Rossby number for Mars. Tabulate the information that you use and the source of the information. Estimate the widths of the Hadley circulation, in degrees of latitude, for Mars.

4. Derive (5.44) from (5.42) and (5.43).